Nuclear Instruments and Methods in Physics Research A 766 (2014) 250–254

Contents lists available at ScienceDirect

Nuclear Instruments and Methods in Physics Research A

journal homepage: www.elsevier.com/locate/nima

Event reconstruction in the RICH detector of the CBM experiment at FAIR

J. Adamczewski [a], K.-H. Becker [b], S. Belogurov [c], N. Boldyreva [d], A. Chernogorov [c], C. Deveaux [e], V. Dobyrn [d], M. Dürr [e], J. Eom [f], J. Eschke [a], C. Höhne [e], K.-H. Kampert [b], V. Kleipa [a], L. Kochenda [d], B. Kolb [a], J. Kopfer [b], P. Kravtsov [d], S. Lebedev [e,*], E. Lebedeva [e], E. Leonova [d], S. Linev [a], T. Mahmoud [e], J. Michel [a], N. Miftakhov [d], Y. Nam [f], W. Niebur [a], K. Oh [f], G. Ososkov [g], E. Ovcharenko [c], C. Pauly [b], J. Pouryamout [b], S. Querchfeld [b], J. Rautenberg [b], S. Reinecke [b], Y. Riabov [d], E. Roshchin [d], V. Samsonov [d], J. Song [f], O. Tarasenkova [d], T. Torres de Heidenreich [a], M. Traxler [a], C. Ugur [a], E. Vznuzdaev [d], M. Vznuzdaev [d], J. Yi [f], I.-K. Yoo [f]

[a] GSI Darmstadt, Germany
[b] University Wuppertal, Germany
[c] ITEP Moscow, Russia
[d] PNPI Gatchina, Russia
[e] University Gießen, Germany
[f] Pusan National University, South Korea
[g] LIT JINR Dubna, Russia

ARTICLE INFO

Available online 9 May 2014

Keywords:
Hough transform
Event reconstruction
Artificial neural network
Ring reconstruction
Ellipse fitting
Circle fitting

ABSTRACT

The Compressed Baryonic Matter (CBM) experiment at the future FAIR facility will investigate the QCD phase diagram at high net-baryon densities and moderate temperatures. One of the key signatures will be di-leptons emitted from the hot and dense phase in heavy-ion collisions. Measuring di-electrons, a high purity of identified electrons is required in order to suppress the background. Electron identification in CBM will be performed by a Ring Imaging Cherenkov (RICH) detector and Transition Radiation Detectors (TRD). In order to access the foreseen rare probes, the detector and the data acquisition have to handle interaction rates up to 10 MHz. Therefore, the development of fast and efficient event reconstruction algorithms is an important and challenging task in CBM. In this contribution event reconstruction and electron identification algorithms in the RICH detector are presented. So far they have been developed on simulated data but could already be tested on real data from a RICH prototype testbeam experiment at the CERN-PS. Efficient and fast ring recognition algorithms in the CBM-RICH are based on the Hough Transform method. Due to optical distortions of the rings, an ellipse fitting algorithm was elaborated to improve the ring radius resolution. An efficient algorithm based on the Artificial Neural Network was implemented for electron identification in RICH. All algorithms were significantly optimized to achieve maximum speed and minimum memory consumption.

1. The CBM experiment

The Compressed Baryonic Matter (CBM) experiment will be a dedicated setup for the measurement of fixed target heavy ion collisions at the future FAIR facility [1]. It is being designed for the investigation of the properties of highly compressed baryonic matter. The research program of the CBM experiment will start with primary beams from the SIS100 synchrotron (protons up to 29 GeV, Au up to 11 AGeV), and will be continued with beams from the SIS300 synchrotron (protons up to 90 GeV, Au up to 35 AGeV). The beam extracted to the CBM cave reaches intensities up to 10^9 Au ions per second. A key item of the CBM physics program is the precise measurement of low-mass vector mesons and J/ψ in their leptonic decay channel. For these studies excellent electron identification in terms of efficiency and purity is required.

The CBM detector setup is shown in Fig. 1. The core detector of CBM is a Silicon Tracking System (STS) consisting of eight Silicon micro-strip detector layers in a magnetic dipole field. The STS

* Corresponding author.
E-mail address: s.lebedev@gsi.de (S. Lebedev).

http://dx.doi.org/10.1016/j.nima.2014.04.082
0168-9002/

detector provides track and vertex reconstruction and momentum determination. Detectors for particle identification will be placed behind the magnet: a Ring Imaging Cherenkov (RICH) detector together with Transition Radiation Detectors (TRD) for electron identification and a time-of-flight (TOF) wall for hadron identification. The setup will be completed by an Electromagnetic CALorimeter (ECAL) and a Projectile Spectator Detector (PSD).

2. The CBM-RICH detector

The RICH detector is designed to provide identification of electrons and suppression of pions in the momentum range below 8 GeV/c. This will be achieved using a gaseous RICH detector built in a standard projective geometry with focusing mirror elements and a photon detector. CO_2 with a pion threshold for Cherenkov radiation of 4.65 GeV/c will be used as radiator gas. The RICH will consist of a 1.7 m long gas radiator at 2 mbar overpressure and two arrays of mirrors and photon detector planes. The mirror plane is split horizontally into two arrays of spherical glass mirrors, 4×1.5 m^2 each. The 72 mirror tiles have a 3 m radius of curvature, and a thickness of 6 mm. Rings of Cherenkov radiation will be projected onto two photon detector planes 2×0.6 m^2 each located behind the CBM dipole magnet and shielded by the magnet yokes. The design of the photon detector plane is based on MAPMTs (e.g. H8500 from Hamamatsu) with about 55,000 channels in total. In beam tests with a prototype RICH of real-size length showed that 23–24 photons are measured per electron ring (see [2] also for details on the RICH).

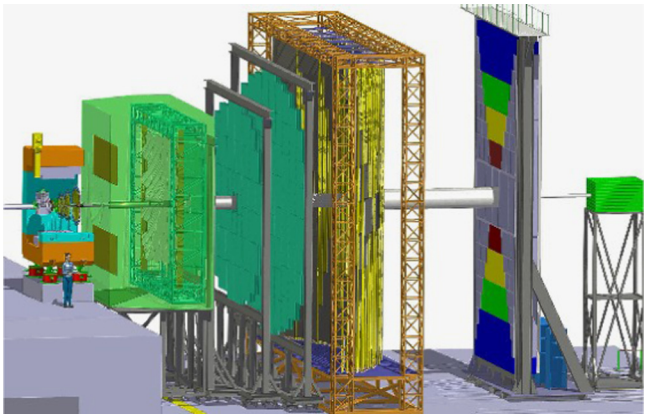

Fig. 1. The CBM experimental setup.

Fig. 2 shows an example of a typical response of the RICH detector to a central Au–Au collision at 25 AGeV beam energy. On average the number of detected photons is around 900 per event. The mean number of particles leaving at least 1 detected photon in the RICH is 65 and 45 with at least 7 detected photons. The largest fraction of recorded photons in the RICH stems from $e^{\pm}$ from γ-conversions in the STS or the magnet yoke (37 rings per event). This material budget significantly increases the ring density in the RICH and causes many overlapping rings. The hit distribution on the photon detector planes is not uniform, but increases in the inner part up to 0.5 hits/cm^2 per event.

3. Event reconstruction in the CBM-RICH detector

Event reconstruction in the RICH detector includes three steps (see Fig. 3). First, reconstructed STS tracks are extrapolated to the mirror. These tracks are then reflected onto the photon detector

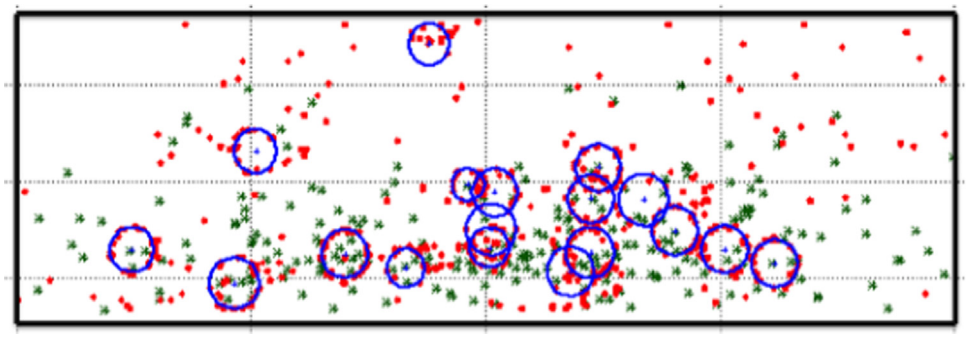

Fig. 2. Simulation of typical response of the upper photon detector plane of the RICH detector to a central Au–Au collision at 25 AGeV beam energy. Blue circles: reconstructed rings; red points: RICH hits including noisy channels (0.35%); green markers: reconstructed track projections onto the photon detector plane. (For interpretation of the references to color in this figure caption, the reader is referred to the web version of this paper.)

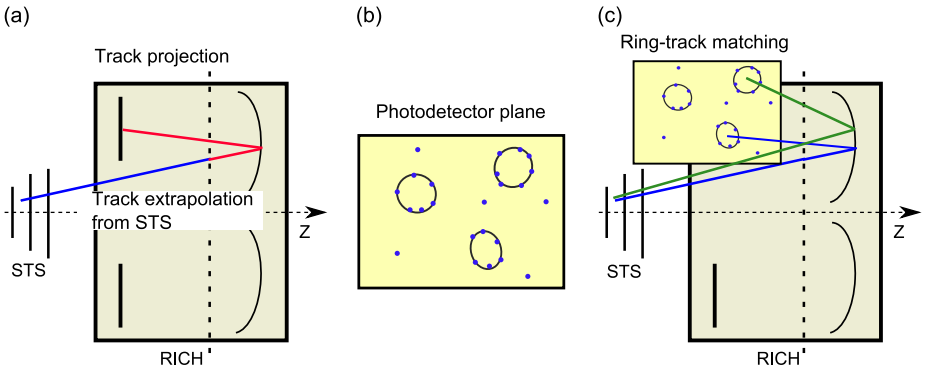

Fig. 3. Three steps of the event reconstruction in the RICH detector. (a) STS track extrapolation and projection onto the photon detector plane; (b) the photon detector plane with hits and reconstructed rings; (c) RICH ring and STS track matching.

plane providing track positions in the plane. Rings are searched for as described below, finally grouping certain hits to a ring. A further ring or ellipse fit provides more precise values of its radius and center. The last step is to match the found rings with the extrapolated STS tracks and identify particles using the ring radius and the momentum information.

3.1. Ring reconstruction algorithm

The developed ring recognition algorithm [3–5] is a standalone process, as input is only an array of RICH hits and no track information are used. The ring search is based on the Hough Transform [6] where hit triplets are combined and the corresponding ring parameters are calculated because each combination of three hits defines a ring. The main disadvantage is that in its straight-forward realization for a multi-parametric curve recognition the HT requires very large combinatorics which makes it intrinsically slow. The method can be optimized by making use of the limited maximum radius R_{max} for Cherenkov rings in the CBM-RICH detector. Thus, instead of combining all possible hit triplets in the whole photon detector plane, only hits within a local area around a possible ring candidate are combined. As illustrated in Fig. 4 only hits are combined which lie within a predefined region around the initial hit. Then ring center and radius are calculated using HT equations from every triplet of selected hits and the corresponding Hough histograms (ring center, radius) are filled. Strong peaks in the Hough histograms should correspond to the expected ring center and radius. If the peak is higher than a prescribed cut this ring-candidate is accepted and shifted to the ring-candidate array, otherwise rejected. Found rings are fitted as circle using an implementation of the COP (Chernov–Ososkov–Pratt) [7] algorithm which offers very high computational speed.

In this step also fake rings are found which are formed by random combinations of hits. Such fake rings are a frequent problem in particular in regions of high ring density with overlapping rings. Therefore the ring search is followed by a quality check in which a quality parameter is calculated by an artificial neural network from six input parameters: number of hits in the ring, ring radius, χ^2 of the circle fit, ring position on the photon detector plane, uniformity of the hit distribution around the ring, and the number of hits in a small corridor around the ring fit. For each ring-candidate the algorithm also checks for shared hits with all other ring-candidates. If the candidate shares more than 25% of its hits with a better quality ring the candidate is rejected.

Due to the geometrical layout of the RICH detector, the ring radius of high quality rings varies slightly from 4.3 cm to 5.2 cm depending on the position of the photon detector plane (see Fig. 5, left). The right plane of Fig. 5 shows the distribution of the fitted radius for $e^{\pm}$ located in a small area on the photon detector plane. The local ring resolution is 0.08 cm (1.6%) which compares well with results from the RICH prototype test (1.3%). The rings also have a slight elliptic shape because the photon detector plane is only approximately placed in the focal plane. To further improve the ring parameter determination, an ellipse fitting algorithm based on the Taubin method [8] is applied as last step which allows to describe the ring shape more precisely.

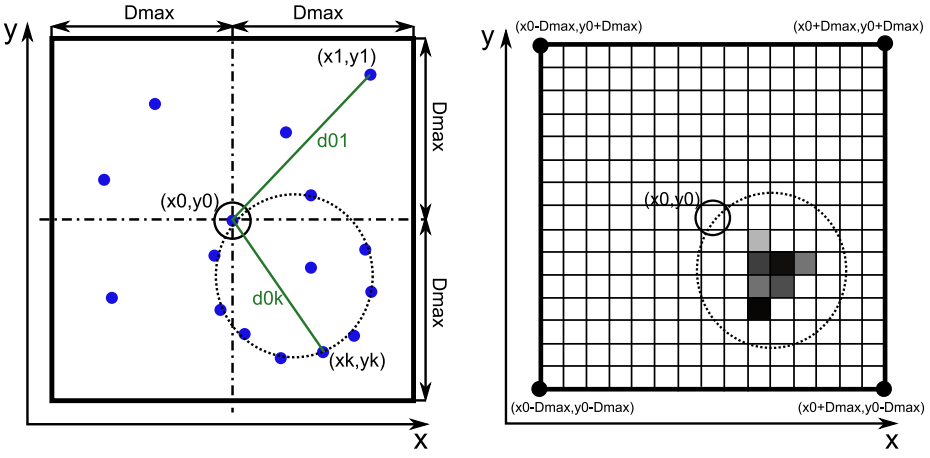

Fig. 4. Left: Illustration of local ring search. Right: Schematic view of the two dimensional histogram of ring centers.

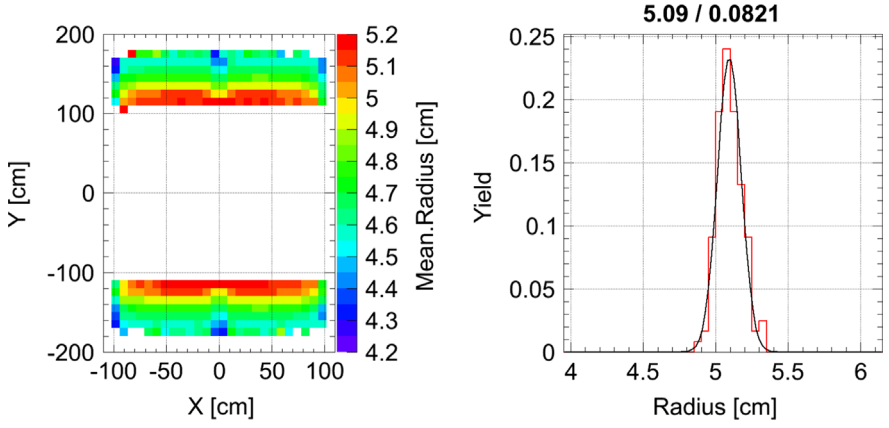

Fig. 5. Left: Mean value of the fitted radius of $e^{\pm}$ from the target in dependence on the ring position on the photon detector plane. Right: Fitted radius for rings located in a small area on the photon detector plane. The histogram is fitted by a Gaussian, numbers on top represent mean and sigma of the Gaussian fit.

3.2. Electron identification algorithm

After the ring reconstruction procedure rings are matched to reconstructed tracks from the STS detector which have been extrapolated to the RICH photon detector plane. The matching is done by selecting the shortest distance between ring centers and extrapolated tracks. For correctly found and matched rings this distance peaks around 0.2 cm. The majority of fake ring-track combinations have distances larger than 1 cm. Such combinations are typically caused by rings from secondary electrons which leave no track in the STS and pion tracks originating in the primary vertex. For pions with momenta below the Cherenkov threshold this is the only source of pion misidentification.

The electron identification algorithm in RICH is based on an artificial neural network (ANN). Nine input parameters have been chosen which allow to separate electrons and pions successfully: major and minor semi-axes of the ellipse fit, rotation angle of ellipse, radial angle and radial position of the ring, χ^2 of ellipse fit, number of hits, distance to the closest track, momentum of the track. These input parameters are all scaled to the range [0,1] and one output value is derived from the ANN. Electron identification is then performed by cutting on the ANN output value requiring a certain identification efficiency, e.g. 90%.

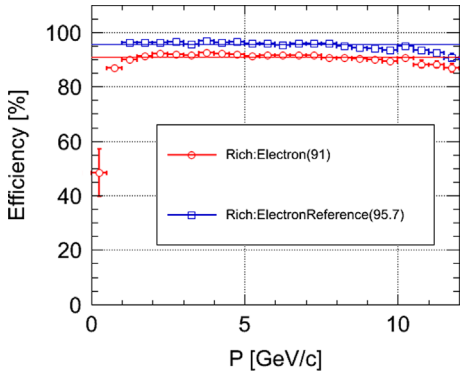

Fig. 6. Ring reconstruction efficiency for primary $e^{\pm}$ (red circle) and primary reference $e^{\pm}$ (blue square) in dependence on momentum. Simulation was performed for central Au–Au collisions from UrQMD at 25 AGeV beam energy. Horizontal lines represent numbers integrated over momentum. (For interpretation of the references to color in this figure caption, the reader is referred to the web version of this paper.)

4. Results from simulation studies

All results presented in this section are based on simulation studies performed for central Au–Au collisions from the Ultrarelativistic Quantum Molecular Dynamics model (UrQMD) [9] at 25 AGeV

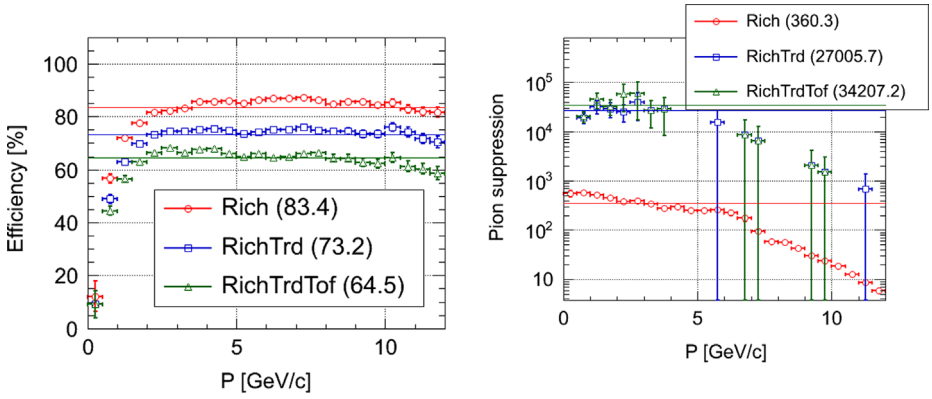

Fig. 7. Left: Electron identification efficiency in dependence on momentum. Right: Pion suppression factor in dependence on momentum. Colors represent different reconstruction steps and detectors which are used for the electron identification: RICH (red circle), RICH+TRD (blue square) and RICH+TRD+TOF (green triangle). Horizontal lines represent numbers integrated over momentum. (For interpretation of the references to color in this figure caption, the reader is referred to the web version of this paper.)

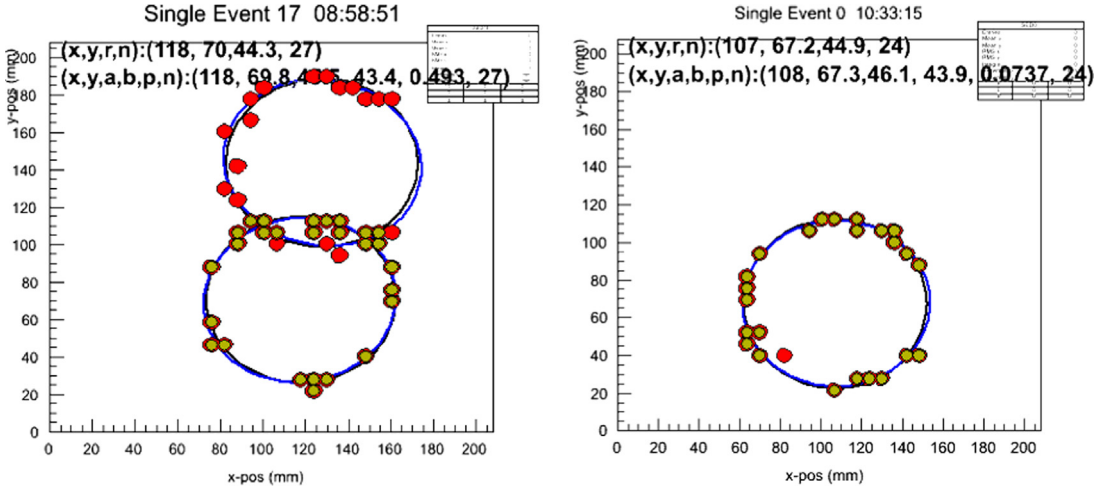

Fig. 8. Example events from RICH prototype data.

beam energy. In order to enhance statistics and investigate the RICH response to primary electrons, $5e^+$ and $5e^-$ were embedded into each UrQMD event at the primary vertex.

Fig. 6 shows the ring reconstruction efficiency for electrons in dependence on momentum. Results are presented for rings from primary $e^\pm$ with at least seven detected photons and rings from for the so-called primary reference $e^\pm$ which have more than 15 detected photons in the ring and a momentum larger than 1 GeV/c. The ring reconstruction efficiency integrated over the momentum range from 0 to 12 GeV/c is 91% for primary $e^\pm$ and 95.7% for the reference set. The calculation time of the algorithm is about 45 μs per event for one CPU core (2.3 GHz Intel Core i7, I/O not included in the calculation time).

Fig. 7 shows the electron identification efficiency and the pion suppression factor in dependence on momentum. The pion suppression factor is defined as the number of pions which can potentially be identified as electron (reconstructed track in STS, track projection in RICH photon detector plane, about $308\pi^\pm$ per event) divided by the number of pions identified as electrons. Overall, a mismatch of pion tracks with rings from secondary electrons leaving no track in the STS is the dominant source of pion misidentification in the RICH detector. The RICH detector alone yields a pion suppression factor of 360 at an electron identification efficiency of 83% for momenta below 12 GeV/c. In combination with TRD and TOF a factor 34,000 is reached at 64.5% electron identification efficiency. This level of pion suppression fully satisfies the requirement of a factor 10,000 as required by physics feasibility studies and would even allow to release some cuts on electron identification resulting in higher efficiencies.

5. Full-size RICH prototype

To verify the concept of the CBM-RICH detector a real-size prototype was constructed and tested at the PS/T9 beam line at CERN in 2011 and 2012 [2]. Data from this prototype allowed to validate the CBM-RICH simulations with the CbmRoot framework. In particular the ring reconstruction and the fitting algorithms described above could be tested on real data.

Ring reconstruction and fitting are done as described above. In order to estimate the electron ring finding efficiency, events are selected based on information from two threshold Cherenkov counters located in front of the RICH prototype and an electromagnetic calorimeter placed in the back. The ring finding efficiency is then defined as the number of events in which at least one ring was found divided by the number of events with at least one detected photon. The quality of reconstructed rings was checked for a limited sample using the event display as shown in Fig. 8.

Fig. 9 shows the ring reconstruction efficiency (black line) in dependence on the number of hits per event. The integrated efficiency is 99.1%. The ring fitting efficiency is evaluated assuming

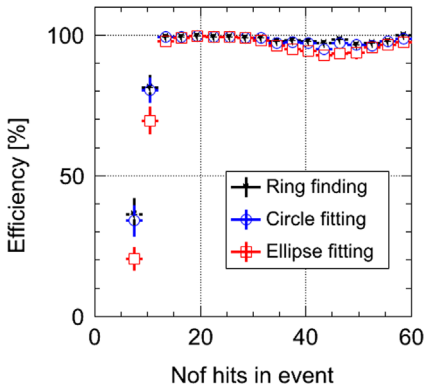

Fig. 9. Efficiency of the ring reconstruction, circle fitting and ellipse fitting in dependence on the number of hits per event for electrons at 3 GeV/c momentum. (For interpretation of the references to color in this figure caption, the reader is referred to the web version of this paper.)

that a ring is correctly fitted by the circle fitter if its radius belongs to a range 3–6 cm corresponding to a wide interval around the mean radius of electron rings (4.5 ± 1.5 cm). For the ellipse fitter, major and minor halfaxes are required to lie in the same range. The fitting efficiency is defined as the number of correctly fitted rings divided by the number of events with at least one detected photon. The efficiency of the circle (blue line) and ellipse (red line) fits is shown in Fig. 9 both lying close to 100%. In summary, the developed ring finding and fitting routines were successfully tested with real data and good agreement of ring properties in simulation and data could be found.

Acknowledgments

This work was supported by the Hessian LOEWE initiative through the Helmholtz International Center for FAIR, by the GSI F&E-Cooperation with Gießen and Wuppertal (WKAMPE1012), by BMBF Grants 05P12RGFCG, 05P12PXFCE and 05P09PXFC5, by the National Research Foundation of Korea (2012004024), and by Helmholtz Grant IK-RU-002 and SC ROSATOM through FRRC.

References

[1] B. Friman, et al., (Eds.), The CBM Physics Book, Springer, 2011.
[2] C. Pauly, et al., The CBM RICH project, these proceedings.
[3] S. Lebedev, et al., Journal of Physics: Conference Series 219 (2010) 032015.
[4] S. Lebedev, et al., Journal of Physics: Conference Series 396 (2012) 022029.
[5] S. Lebedev, et al., in: PoS ACAT2010 060, 2010.
[6] P.V.C. Hough, Method and Means for Recognizing Complex Patterns, US Patent 3,069,654, 1962.
[7] G. Ososkov, N. Chernov, Computer Physics Communications 33 (1984) 329.
[8] N. Chernov, Journal of Mathematical Imaging and Vision 27 (2007) 231.
[9] S. Bass, et al., Progress in Particle and Nuclear Physics 41 (1998) 255.